Using Mimics to understand fluid-structure interaction at small scale in complex geometries

Irfan Khan, Cyrus Aidun
G.W. Woodruff School of Mechanical Engineering,
Georgia Institute of Technology,
Atlanta, GA.

Abstract

Problems in fluid-structure interaction at small scale occur in applications related to bioengineering, micro-electromechanical systems and manufacturing processes. Due to the small scale and complex nature of the geometry, experimental investigations are limited in their effectiveness. Thus research in this area is dependent mainly on analytical and numerical investigations. However the complex nature of the geometry in addition to limitations existing in numerical techniques available in commercial codes promoted the use of major approximations both in the assumptions about the geometry and the necessary constitutive relations for closure in the problem. These assumptions prevented a comprehensive understanding of the physics of the phenomena.

In paper industry there is considerable interest in understanding the fluid-structure interaction problem occurring in the process of wet-pressing. Because of the high volume manufacturing process of paper making, even a small increase in the efficiency of de-watering leads to significant savings in total energy cost. In this work a numerical tool based on a hybrid Lattice-Boltzmann Finite Element method has been developed to understand fluid-structure interaction in complex geometries. The image analysis software MIMICS has been used to obtain the solid model of the actual geometry called felt. This paper discusses the progress made in this direction.

Introduction

Problems where fluid and solid interact dynamically at small scales occur in various engineering and biomedical applications. Flow of blood in biological systems, micro-electro-mechanical systems like lab-on-chip and ink-jet processes and flow in deformable porous media as occurring in paper manufacturing are some example of such applications.

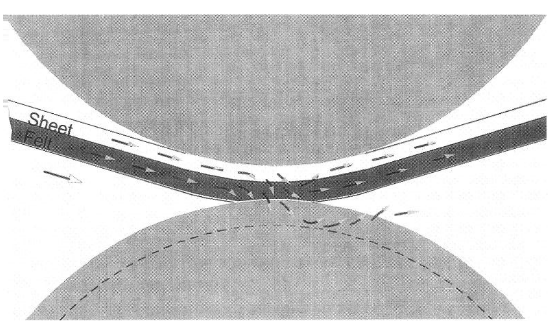

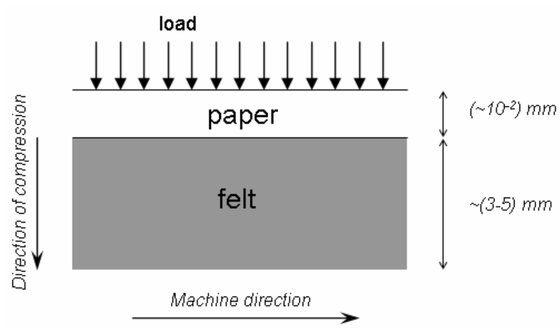

a ***b***

Figure 1a: Pictorial representation of water removal during wet-pressing.
b: Paper-felt system, showing machine direction and direction of compression

In the process of wet-pressing, that occurs during paper manufacturing, continuous sheets of wet paper web and felt pass through rollers or a roller and a die, as shown in Figure 1. Water in the paper web is squeezed partially into the felt and partially out of the system. Subsequently the moist paper passes through a series of heated rollers where the rest of the water is removed through vaporization.

The goal of wet-pressing is to remove as much water from the paper web as possible without affecting the quality of paper. The dryness of the sheet is usually measured either by the percent solid in the paper or by the moisture ratio. Typically the process of wet-pressing removes 45-50% of water from the wet paper. Drying removes 30-40% of water. The completely formed paper has 5-7% of moisture in it.

Process	*% solids at end of process*	*Energy/Kg of water removed*
Pressing	45-50	2.786 KJ/Kg
Drying	85-93	2257 KJ/Kg (latent heat of vaporization)

Table 1: Compares the process of pressing and drying in terms of solids removed and cost per gram of water removed.

As can be seen in the above Table 1, the cost of removing water in the drying stage is expensive because of the energy intensive process of vaporization. Energy spend in drying can be reduced if water is removed more effectively during pressing. It is important to note that due to the high volume process of paper making, even a small increase in the efficiency of wet-pressing can lead to significant reduction in total energy cost. Figure 2 shows the effect of increasing the ingoing solids on the cost of drying. As can be seen, an increase in the solids by 5% (50 to 55) going into the drying section, leads to a reduction in cost per ton of drying by $20. When accumulated over an entire year this may lead to millions in savings.

Figure 2: Effect of ingoing sheet moisture on cost of drying

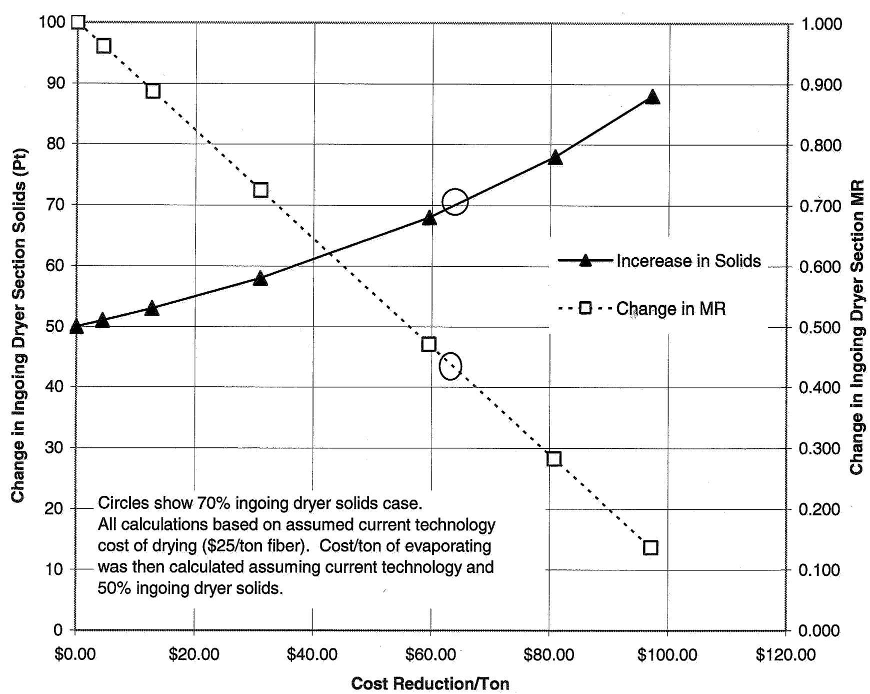

Consequently the process of pressing has been studied extensively. The studies have concentrated mostly on the physics in the paper web. The aim being, to determine the optimum pressing regime to improve the efficiency of de-watering during pressing.

Experimental studies performed by Wahlstrom [1960], Nilesson & Larson [1964], Busker [1980] and Busker et al [1984] helped in further understanding the process qualitatively. These investigations led to the understanding of different phases in the process of pressing. Figure 3 shows the four phases during the process of pressing as described by Nilesson & Larson [1964]. However, the high machine speed (~ 10 ms^{-1}), low residence time ((~ 10^{-2} s) and small length scales ((~ 10^{-4} m) limited the effectiveness of the experimental data for industrial application.

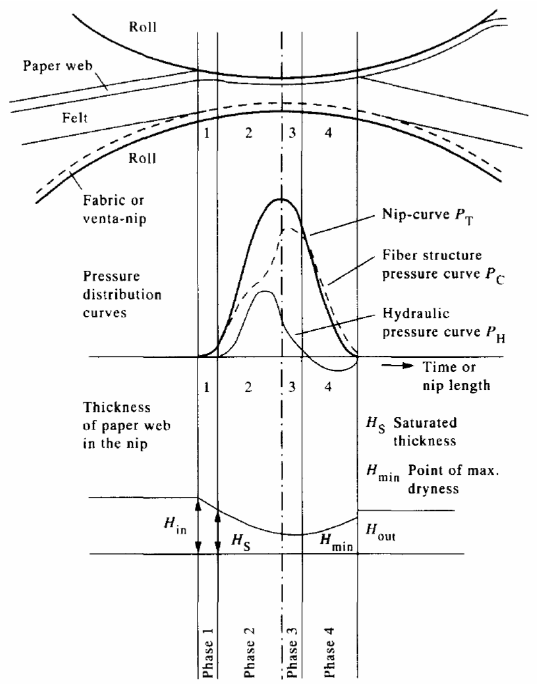

Figure 3: The 4 phases in the process of pressing as described by Nilsson & Larson [1964].

The problem was investigated with analytical and numerical methods by Kataja et al [1992], Jonsson et al [1992, 1992],Velten et al [2000], Bezanovic et al [2006, 2007, 2007]. They used homogenization principles along with assumptions about the constitutive relations about the solid and fluid to reduce the problem for one-dimensional analysis. However in reality the felt structure is highly non-homogeneous and the newer felt design necessitates a variation in felt porosity. The lack of a comprehensive understanding of the various parameters on the deformation and de-watering of felts has meant that the design have been based on a qualitative understanding.

In an attempt to understand wet-pressing, this research work tries to understand deformation of porous media under externally applied load and the effect of fluid inside it. In order to answer some of the questions posed above, it becomes imperative to model pressing as a three-dimensional problem along with modeling the heterogeneity of the porous media. However, the complex nature of the geometry and the small time scale require high spatial and temporal resolution leading to large computational load. Thus efficient numerical tools need to be chosen.

For modeling fluid flow, the Lattice-Boltzmann method has evolved as an attractive alternative. The accuracy of Lattice-Boltzmann method has been shown to be comparable to traditional numerical methods like Finite-Volume, Finite-Difference and Finite-Element [Noble et al (1996); Bernsdorf et al (1999), Breuer (2000)]. Further, for solving flows in complex geometries like porous media, the Lattice-Boltzmann method has proved to be more efficient than traditional methods [Bernsdorf et al (1999)]. Because of the local nature of the calculations, the method is amenable to distributed computing. This use of LBM is critical in this research work, as the size of the computational domain turns out to be very large, one that cannot be efficiently solve using serial computing. In this research work, a LBM with single-relaxation BGK model as implemented in Aidun et al (1998) has been used.

In this work, as a first approximation, a linear elastic model has been used for simulating the deformation of the felt geometry. In reality, the felt material shows a partial plastic behavior in the first stage of pressing. In subsequent stages the behavior is more close to elastic (Velten et al (2000); Beck (1983)]. However during the compression phase, the material behaves as elastic for all practical purposes. The Finite Element method with 4-node linear quadrilateral elements have been used to discretize the geometry and form the weak system. The reason for using Finite Element method for modeling the deformation of the solid phase is because of its robustness and accuracy. Further there has been progress in development of efficient parallel iterative schemes [Saad (1996)] that make the solution of solid phase easy. Also with the improvements in meshing algorithm, it is now trivial to mesh a complex geometry such as the felt.

In the following, details have been provided regarding the procedure for geometry reconstruction. Additionally the Lattice-Boltzmann Finite-Element technique is outlined with information on parallelizing the code and running on large clusters. Finally results of some validation studies and sample simulation run on actual geometry are provided.

Methodology

Geometry Reconstruction

A sample of porous felt is shown in Figure 4. In order to perform a finite element analysis of the deformation and Lattice-Boltzmann analysis of flow through the geometry, a solid model of geometry needs to be obtained. In the following a brief outline of the procedure for reconstructing the solid model from the sample is given.

X-ray Microtomography was used to obtain images of the sample at specified intervals as show in Figure 5a. In this case the sample was a 3mmx3mmx3.15mm piece of drying felt. The

Figure 4: Image of felt sample provide used in wet-pressing.

images were taken at an interval of 3.5 microns. This was done using skyscan 1072.

By selecting the appropriate pixels from all the images and using them to generate voxels, a three-dimensional geometry can be created. This process consists of thresholding, region growing and 3D reconstruction. Further surface smoothing algorithms and triangle quality improvement algorithms can be used to improve the quality of three-dimensional solid model for FEA analysis. Materialize's MIMICS package was used to carry out the above operations for constructing the solid model from X-ray Microtomography images.

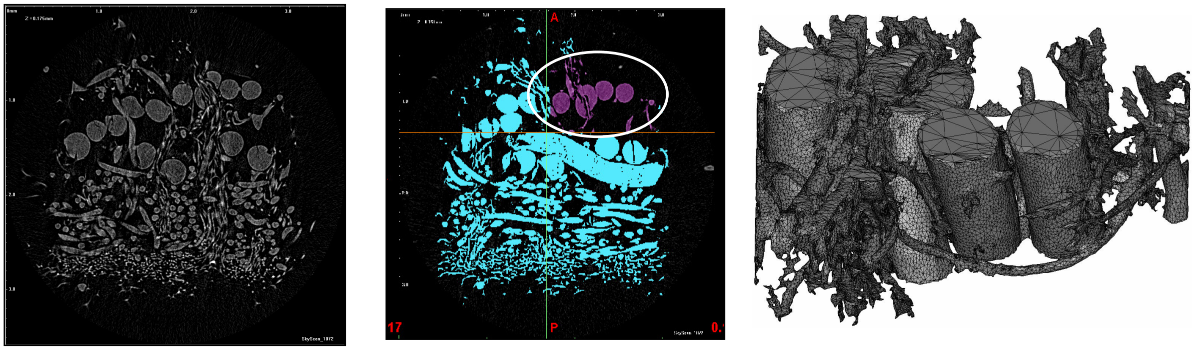

Figure 5: (a) X-ray Microtomography image of felt sample; (b) Using thresholding, region growing and isolation on pixels; (c) three-dimensional mesh of the solid model generated from images

Lattice-Boltzmann Method

The Lattice-Boltzmann method (LBM) is based on a specialized discretization of the continuous Boltzmann equation. As such, it is a kinetic model that models the fluid phase at a mesoscopic level.

Just as its predecessor the lattice-gas automata, the LBM starts with an initial lattice where particles residing at each lattice node evolve in time based on certain rules. During this process the particles propagate and collide with other particles. The average motion of the particles describes the macroscopic behavior of the system.

In LBM, the state of the fluid is defined by a single-particle distribution function $f_{\sigma i}(\boldsymbol{r},t)$ indicating the probability of finding a particle at $\boldsymbol{r}$ and time t. At each time step the particles propagate to the neighboring lattice along discrete velocity vectors $\boldsymbol{e}_{\sigma i}$. The dynamics of propagation are governed by the following lattice-Boltzmann equation. The method is implemented based on Aidun et al [1998]

$$f_{\sigma i}(\boldsymbol{x}+e_{\sigma i},t+1)-f_{\sigma i}(\boldsymbol{x},t)=-\frac{1}{\tau}\left[f_{\sigma i}(\boldsymbol{x},t)-f_{\sigma i}{}^{eq}(\boldsymbol{x},t)\right] \tag{1}$$

Where τ is the relaxation parameter. It can be set to obtain the appropriate viscosity, as given in the following equation.

$$\upsilon=\frac{(2\tau-1)}{6} \tag{2}$$

The equilibrium distribution $f^{eq}{}_{\sigma i}(\boldsymbol{r},t)$ is given as,

$$f_{\sigma i}{}^{eq}(\boldsymbol{x},t)=\rho(\boldsymbol{x})\left[A_{\sigma}+B_{\sigma}(e_{\sigma i}\cdot\boldsymbol{u}\right] \tag{3}$$

where the coefficients of the equilibrium equation A_σ B_σ C_σ and D_σ are derived based on the conservation laws of mass, momentum and energy. The hydrodynamic fields, mass density ρ, momentum density $\rho\boldsymbol{u}$ and the momentum flux given as $\rho\boldsymbol{I}+\rho\boldsymbol{uu}$ are given as follows

$$\rho = \sum_{\sigma} \sum_{i} f_{\sigma i}(\boldsymbol{x}, t), \tag{4}$$

$$\rho \boldsymbol{u} = \sum_{\sigma} \sum_{i} f_{\sigma i}(\boldsymbol{x}, t)\, \boldsymbol{e}_{\sigma i}, \tag{5}$$

$$\rho \boldsymbol{I} + \rho \boldsymbol{u}\boldsymbol{u} = \sum_{i} f_{i}(\boldsymbol{x}, t)\, \boldsymbol{e}_{i}\, \boldsymbol{e}_{i} \tag{6}$$

Finite Element Method

The deformation of the porous media has been idealized using a linear elastic model. Cauchy's equation governs the trajectory and deformation of an elastic deformable solid.

$$\partial_j \cdot T_{ij} + \rho g_i = \rho \ddot{u} \tag{7}$$

The geometry has been discretized using 4-node linear tetrahedral elements. The meshing was done using MIMICS's FEA module. Within each element the deformation is approximated using linear Lagrangian shape functions. The resulting weak system of equations is given by the following equation.

$$M\ddot{\boldsymbol{u}} + C\dot{\boldsymbol{u}} + K\boldsymbol{u} = \boldsymbol{F} \tag{8}$$

Where $\boldsymbol{u}$ is the deformation vector, $\boldsymbol{M}$, $\boldsymbol{C}$ and $\boldsymbol{K}$ are the mass, damping and stiffness matrices respectively. Newmark's method is used to integrate the above 2nd order system of equations in time. According if u_t is the deformation at time t and u_{t+1} is the deformation at time t+1 then the above system of equations modifies to

$$\left[K + \frac{\gamma}{\beta \Delta \boldsymbol{t}} C + \frac{1}{\beta \Delta \boldsymbol{t}^2} M\right] \boldsymbol{u}_{t+1} = f_{t+1} + C\left[\frac{\gamma}{\beta \Delta \boldsymbol{t}} u_t + \left(\frac{\gamma}{\beta} - 1\right)\dot{u}_t + \left(\frac{\gamma}{2\beta} - 1\right)\Delta \boldsymbol{t} \ddot{u}_t\right]$$
$$+ M\left[\frac{1}{\beta \Delta \boldsymbol{t}^2} u_t + \frac{\gamma}{\beta \Delta \boldsymbol{t}} \dot{u}_t + \left(\frac{1}{2\beta} - 1\right)\ddot{u}_t\right] \tag{9}$$

$$\ddot{\boldsymbol{u}}_{t+1} = \beta_n^{-1} \Delta t^{-2} [\boldsymbol{u}_{t+1} - \boldsymbol{u}_t - \frac{1}{\beta \Delta t} \dot{\boldsymbol{u}}_t - \Delta t^2 (\frac{1}{2\beta} - 1)\ddot{\boldsymbol{u}}_t] \tag{10}$$

$$\dot{\boldsymbol{u}}_{t+1} = \dot{\boldsymbol{u}}_t + \Delta t[(1 - \gamma_n)\ddot{\boldsymbol{u}}_{t+1} + \gamma_n \ddot{\boldsymbol{u}}_{t+1}] \tag{11}$$

Here β and γ are Newmark's constant. The resulting system of equations is solved using iterative schemes.

Fluid-Solid Coupling

Transfer of forces between fluid and solid is affected through the boundary links where a bounce-back boundary condition is applied. The hydrodynamic forces on the moving boundary is calculated using the following equation.

$$F_{\sigma i}^{(B)}(\boldsymbol{x} + \frac{1}{2}\boldsymbol{e}_{\sigma i}, t + \frac{1}{2}) = 2\boldsymbol{e}_{\sigma i'}\left[f_{\sigma i'}(\boldsymbol{x}, t^{+}) - \rho B_\sigma u_b \cdot \boldsymbol{e}_{\sigma i'}\right] \tag{12}$$

Parallel LBM-FEM code

Need for parallel computing

The complex nature of the geometry and the need to capture the flow physics at small scale necessitates the LB and FE meshes to resolve the geometry with sufficient accuracy. In choosing a LB mesh for a given FE mesh, the accuracy with which the force values are transferred between fluid and solid needs to be considered. This introduces a length scale l_{fea} (MecMaccen et al [2009]) which is defined as the ration of average FE edge length to 1 lattice unit. For accurate transfer of forces between LBM and FEM there is a limitation on l_{fea} given as $\{l_{fea} > 2.5\}$. This implies that the resolution of LB mesh is dependent on the average edge length of FE mesh.

On the analysis void distribution analysis of the geometry it is found that the average pore size is about 0.02 mm. In order to resolve the pores accurately a FE mesh with minimum edge length of 0.005mm is chosen. Note that this edge length is 4 times smaller than the average pore size; thus approximately 4 linear quadrilateral elements can be used to resolve the average pore. Taking the limitation of LB mesh into account from the l_{fea} ratio, we conclude that 1 LB length unit should equal 0.002mm. Based on this correlation the size of LB mesh, memory required and thus computational resources required were extrapolated. Table 3 gives this information.

Size of Geometry x10^{-2} mm	*Total Lattice Nodes*	*Memory Required*	*Computational units*	
			***4**GB/node*	***8**GB/node*
0.2x0.2x0.2	100x100x100	0.8 GB	1	1
1x1x1	500x500x500	93 GB	24	12
3x3x3	1500x1500x1500	2514.5 GB	630	315

Table 3: Memory and computational requirements of the Lattice-Boltzmann code for a given domain size.

Further the above estimations do not involve the memory requirement for FEA analysis. It is expected that for an FEA analysis the memory requirement are only a fraction of that of LBM. Thus a problem of this magnitude would require massively parallel computing resources to attempt a solution in realistic time frame.

In this research work the following parallel computing resources have been and would be used to carry out the intended simulations.

1. IBM IA-63 linux cluster (Mercury)
   1,774 Intel Itanium 2 1.3/1.5 GHz processors, 4 GB to 12 GB memory/node
   Peak performance: 10.23 TF (7.22 TF sustained)
2. Dell 1950 compute nodes (Steele),
   840 dual quad-core 64-bit Intel 2.33 GHz E5410 CPUs with 16 GB or 32 GB of RAM.
   Peak Performance: 62.63 TFLOPS
3. TACC Sun Visualization Cluster (Spur)

128 compute cores, 2.33 GHz AMD opteron and 32 NVIDIA FX5600 GPUs.

Parallelizing LBM-FEM code

The compute nodes used to carry out the LBM calculations (Fluid-CPUs) are different from the compute nodes used for FEA calculations (Solid-CPUs). At each time-step the Fluid-CPUs need the current location and velocity of FEA nodes and similarly the Solid-CPUs need the current forces on FEA nodes. This information is communicated between the Fluid-CPUs and Solid-CPUs through the use of efficient data structures and functions for storing and communicating information. The code is tightly coupled with PETSc (Balay et al [1997]) which provides the necessary data structures and functions for scientific high performance computing.

Parallelizing the LBM code

According to the Lattice-Boltzmann equation (1), the distribution function at lattice node x and time t+1 is solely dependent on the distribution function at lattice x+ei and at time t. This means that there is no need for assembly and solution of equations. Such local nature of algorithm should benefit from a "data-parallelism" approach.

Data-Parallelism is achieved by dividing the domain among the available processors also called ranks. As shown in Figure 6, upon the division of domain, an extra layer of cells also called ghost cells are added to each sub-domain. These ghost cells facilitate the transfer of information between each sub-domain at every time-step, thus maintaining the continuity of the entire domain.

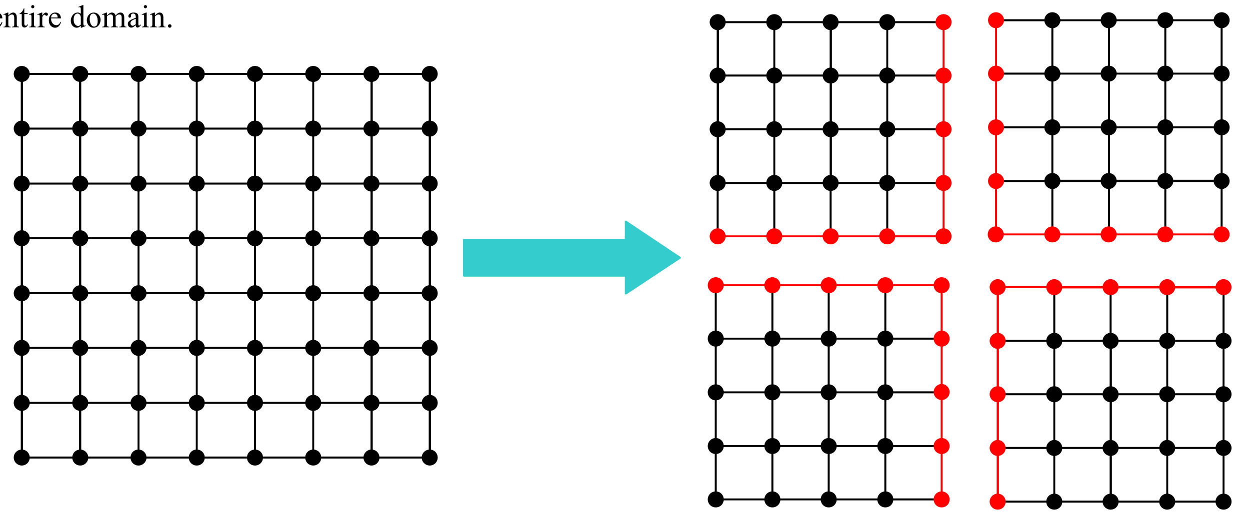

Figure 6: Division of a Lattice-Boltzmann domain into 4 sub-domains. The nodes in black are regular nodes and nodes in red are ghost nodes.

Preliminary Results

Flow simulation

The effects of fluid flow inside the felt geometry were determined using a flow simulation of the geometry as shown in Figure 7. The boundary conditions are as shown in figure 9. A parabolic inlet velocity was used and the geometry was placed inside a rectangular channel with walls. The outlet was set to shear-free boundary condition.

Figure 7: Set up and boundary conditions for simulating flow over the porous geometry.

The resulting normal stress and shear stress distributions on the geometry are as given in the following figure.

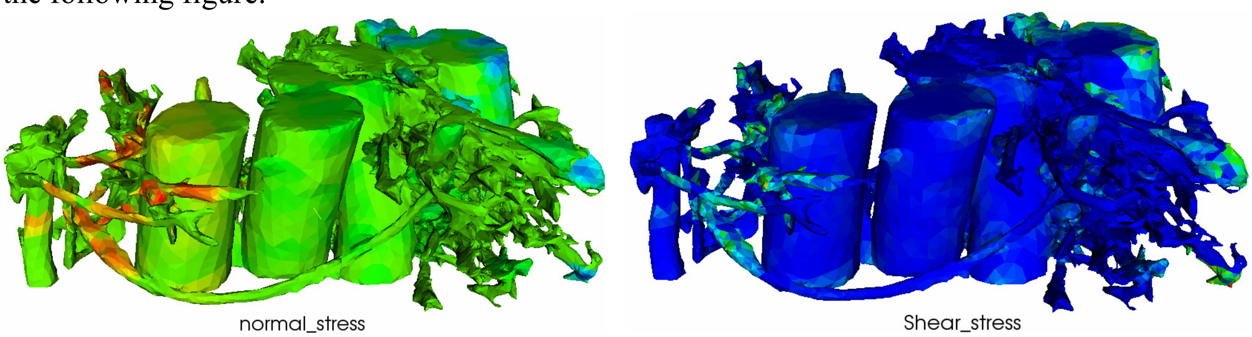

Solid deformation

A smaller sized geometry was used to simulate deformation of the solid. Figure 8 shows the geometry and the applied loads on the left and the resulting deformation on the left. Though the developed numerical technique can also calculate stress and strain distribution resulting from the applied loads, for the analysis of wet-pressing it is sufficient to analyze just the deformation.

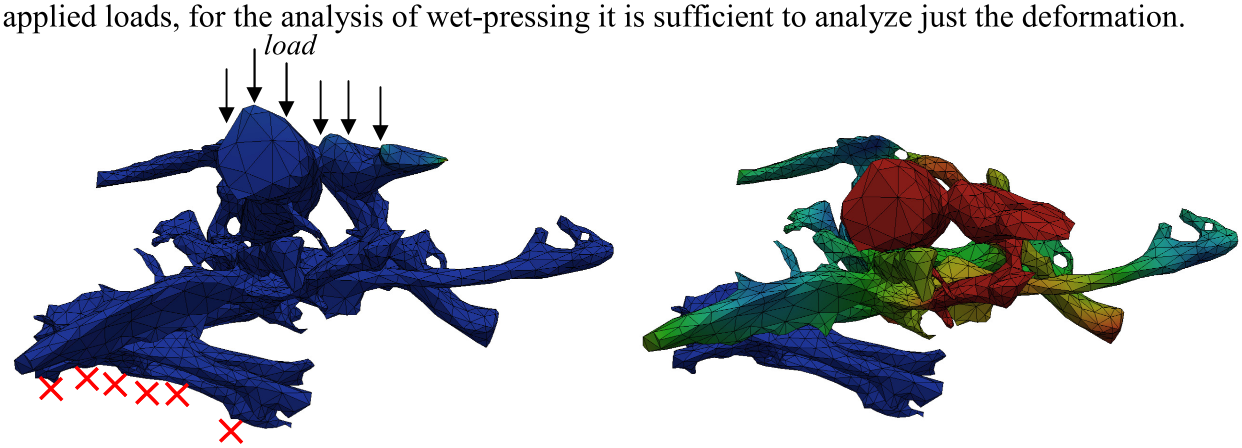

Figure 8: Deformation of solid geometry, boundary conditions specified on left. On right the resulting deformation color scale represents extent of deformation.

Effect of pore distribution

A significant research goal of this work is to understand the effect of pore size distribution in the felt on its deformation and de-watering characteristics. The experimental research done by Busker et al [1984] concluded that felts with high permeability and low compressibility will lead to higher de-watering efficiency. However, felts with high permeability lead to decrease in paper quality. This resulted in variation in felt permeability in the direction of thickness. By making use of various felt geometries used in paper industry we intend to look at the effect of variation in felt permeability in dewatering efficiency.

We hope to make use of the features available in Mimics's "pore analysis module" to accomplish this task. Since the module allows the use of any geometry in the form of an STL file for pore analysis, the goal is to look at variation in pore distribution as the felt deforms.

(More results expected here soon)

Impact and Significance of Proposed Research:

At the core of the present research work is the development of a numerical tool that can be used to model fluid-structure interaction in complex geometries. The use of LBM for modeling fluid phase and FEM for the solid phase lends a number of unique features as already described earlier, for modeling such problems. The ability to make use of parallel computing resources with efficient scaling in fluid-structure interaction problems is a novel achievement in this area. Thus this numerical tool provides the capability of solving larger problems in this field that have not been attempted before.

The findings from the second part of the research work are critical for understanding the dewatering of felt. Better void fraction variation in the felt could lead to better dewatering of felt and pulp system during wet pressing. Even a small improvement in dewatering efficiency can lead to significant improvement in the energy efficiency for the paper industry.

References

[1] Aidun, C.K., Lu, Y. & Ding, E.J. 1998 Direct analysis of particulate suspensions with inertia using the discrete Boltzmann equation. *J. Fluid Mech*. 373, 287–311.

[2] Aidun, C.K. & Lu, Y. 1995 Lattice Boltzmann simulation of solid particles suspended in fluid. *J. Stat. Phys*. 81 (1), 49–61.

[3] Balay S, W. D. Gropp, Lois Curfman McInnes, and Barry F. Smith. Efficient management of parallelism in object oriented numerical software libraries. In E. Arge, A. M. Bruaset, and H. P. Langtangen, editors, Modern Software Tools in Scientific Computing, pages 163–202. Birkhauser Press, 1997.

[4] Beck D., *TAPPI Engineering conference Proceedings* (TAPPI, Atlanta, GA, 1983). pp 475-487

[5] Bernsdorf J., G. Brenner, F. Durst. Numerical analysis of the pressure drop in porous media flow with lattice Boltzmann (BGK) automata. *Computer Physics Communications* 129 (2000) 247–255

[6] Bežanovic, D., van Duijn, C.J., Kaasschieter, E.F.: Analysis of paper pressing: the saturated one-dimensional case. *J. Appl. Math. Mech*. 86(1), 18–36 (2006)

[7] Bežanovic, D., van Duijn, C.J., Kaasschieter, E.F.: Analysis of wet pressing of paper: the three-phase model. Part I: constant air density. *Transport in Porous Media* (2007) 67:93–113

[8] Bežanovic, D., van Duijn, C.J., Kaasschieter, E.F.: Analysis of wet pressing of paper: the three-phase model. Part I: constant air density. *Transport in Porous Media* (2007) 67:171–187

[9] Biot M.A: General theory of three dimensional consolidation, *J. Appl. Phys*. 12, 155–164. (1941)

[10] Breuer M., J. Bernsdorf , T. Zeiser, F. Durst. Accurate computations of the laminar Flow past a square cylinder based on two different methods: lattice-Boltzmann and Finite-volume. *International Journal of Heat and Fluid Flow* 21 (2000) 186-196

[11] Busker, L. H. Wet Press Water Removal Over a Wide Parameter Ranger. *Paper technology and Industry*, 21:3, p91-96, (1980)

[12] Busker, L. H; Cronin. The relative importance of wet press variables in water removal. *Pulp and Paper Canada* 85:6 (1984)

[13] Campbell,W. B. The Physics of Water Removal. *Pulp Paper Mag. Canada* 26, 103-110. (1947)

[14] Chen, S. & Doolen, G.D. 1998 Lattice Boltzmann method for fluid flows. *Ann. Rev. of Fluid Mech*. 30 (1), 329–364.

[15] Durst F., R. Haas, W. Interthal. The nature of flows through porous media. *J. Non-Newtonian Fluid Mech*. 22 (1987) 169.

[16] Ding, E.J. & Aidun, C.K. 2003 Extension of the lattice-Boltzmann method for direct simulation of suspended particles near contact. *J. Stat. Phys*. 112 (3), 685–708.

[17] Ergun S. Fluid flow through packed columns, *Chem. Eng. Prog*., 48(2) (1952) 89-84.

[18] Jonsson K. A. S, Jonsson B. T. L. Fluid Flow in Compressible Porous Media: I: Steady-State Conditions.**v**38, No. 9 *AIChE Journal* (1992)

[19] Jonsson K. A. S, Jonsson B. T. L. Fluid Flow in Compressible Porous Media: II: Dynamic Behavior. **v**38, No. 9 *AIChE Journal* (1992)

[20] Lewalle J, K. M. Singhand J. P. Bambacht. Analysis of the wet pressing of paper pulp. Int. *J. Multiphase Flow* **v**20, No. 2, pp. 415J,37, 1994

[21] Kataja, M., Hiltunen, K., Timonen, J.: Flow of water and air in a compressible porous medium:A model of wet pressing of paper. J. Phys. D: Appl. Phys. 25, 1053–1063 (1992)
[22] Kandhai D., D.J.-E. Vidal, A.G. Hoekstra, H. Hoefsloot, P. Iedema and P.M.A Sloot. Lattice-Boltzmann and finite element simulations of fluid flow in a SMRX static mixer reactor. *Int. J. Numer. Meth. Fluids* **31**: 1019–1033 (1999)
[23] Moller, T. & Trumbore, B. 1997 Fast, minimum storage ray-triangle intersection. *Journal of Graphics Tools* 2 (1), 21–28.
[24] MacGregor, M. A. What happens during shell and groove marking. *TAPPI Jl* 68, 84-91. (1985)
[25] MacMeccan R, Clausen J, Neitzel G, Aidun C. 2009. Simulating deformable particle suspensions using a coupled lattice-Boltzmann and finite-element method. *J. Fluid Mech.* 618:13–39
[26] McNamara, G.R. & Zanetti, G. 1988 Use of the Boltzmann equation to simulate lattice-gas automata. *Phys. Rev. Lett*. 61 (20), 2332–2335.
[27] Nilsson,P. & Larsson,K. O.: Paper web performance in a press nip. *Pulp Paper Mag. Canada* 69, 66-73. (1964)
[28] Noble, D.R., Georgiadis, G.J. & Buckius, R.O., Comparison of accuracy and performance for lattice Boltzmann and finite difference simulations of steady viscous flow. *Int. J. Num. Meth. in Fluids* **v(**23), 1-18 (1996)
[29] Velten, K., Best, W.: Rolling of unsaturated porous materials: evolution of fully saturated zone. *Phys. Rev. E* 62 (3), 3891–3899 (2002)
[30] Wilder, J. E.: The fluid mechanics of plain press nips. *TAPPI J*. 50, 180-186. (1967)
[31] Wahlstrom, P. B. A long term study of water removal and moisture distribution on a newsprint machine press section. Part I. *Pulp Paper Mag. Canada* 61, T379-401. (1960)